Azad Karis

Photoresist thickness examination in photolithography in the manufacturing of transparent displays

Metropolia University of Applied Sciences

Bachelor of Engineering

Biotechnology and Chemical Engineering

Bachelor's Thesis

29 April 2019

Metropolia
University of Applied Sciences

Author Title Number of Pages Date	Azad Karis Photoresist thickness examination in photolithography in the manufacturing of transparent displays 40 pages + 8 appendices 29 April 2019
Degree	Bachelor of Engineering
Degree Programme	Biotechnology and Chemical Engineering
Professional Major	Chemical Engineering
Instructors	Kai Laitinen, Principal Lecturer Anna Ranta, Process Engineer

The goal of this thesis project was to examine whether it is possible to coat a thinner photoresist layer than the one used in the current photolithography process, and to optimize the parameters of the spray coating system. This project was done for Beneq Oy, which is specialized in manufacturing transparent Lumineq displays.

The experimental part of this project mostly concentrated on performing tests of different thickness coated photoresist layers necessary for protecting the aluminum oxide layer during the etching process. Two series of tests with two different photoresist viscosities were conducted and the thickness of the coated layers was examined. The quality of the aluminum oxide layer was inspected after the etching process. The current coated photoresist layer could successfully be decreased by approximately 38 %. Testing with two different dilutions, the role of the solvent was also better understood. Thinner photoresist films were achieved using spray coating with the photoresist of low viscosity and resulted in fewer cavities in the aluminum oxide layer than of higher viscosity.

The optimization of the spray coating system was done using Design of Experiments (DOE) method. In the DOE, a full factorial two-level design was created and performed to evaluate the effects of the factors on the final thickness of the coated photoresist layer. On the basis of the generated model, the speed of the substrates passing in the coating system can be increased by 80 %. More tests should be done to further increase the functionality of the DOE model and the reliability and consistency of the experimental photoresist layer.

The decrease in the thickness of the photoresist layer and the parameter optimization of the spray coating system will result in faster production times, material saving and set potential for further development and investigation for other photolithography process steps. Photoresist coating is the first step in the photolithography process.

Keywords	photoresist, coating, photolithography, etching, DOE

Metropolia
University of Applied Sciences

Tekijä	Azad Karis
Otsikko	Fotoresistin paksuuden tutkiminen läpinäkyvien näyttöjen valmistuksen optisessa litografiassa
Sivumäärä	40 sivua + 8 liitettä
Aika	29.4.2019

Tutkinto	insinööri (AMK)

Tutkinto-ohjelma	bio- ja kemiantekniikka

Ammatillinen pääaine	kemiantekniikka

Ohjaajat	yliopettaja Kai Laitinen prosessi-insinööri Anna Ranta

Insinöörityön tavoitteena oli tutkia, voidaanko optisen litografian prosessissa käyttää ohuempaa fotoresistikerrosta, sekä optimoida pinnoituslaitteiston parametrit. Tämä työ toteutettiin Beneq Oy:lle, joka on erikoistunut läpinäkyvien Lumineq-näyttöjen valmistukseen.

Työn kokeellisessa osiossa tutkittiin substraatin alumiinioksidikerroksen laatua etsausprosessin jälkeen. Substraattien alumiinioksidikerrokset päällystettiin eripaksuisilla fotoresistikerroksilla ja tämän jälkeen tutkittiin, kuinka hyvin fotoresistikerros suojasi alumiinioksidikerrosta. Testit suoritettiin kahtena sarjana ja niissä käytettiin kahta eri fotoresistin viskositeettiä. Tulosten perusteella käytössä oleva fotoresistikerrosta voidaan ohentaa noin 38 %:lla. Pienemmällä fotoresistin viskositeetillä saatiin ohuempia fotoresistikerroksia ja tuloksena oli vähemmän reikiä alumiinioksidikerroksessa etsauksen jälkeen, kuin suuremmalla viskositeetilla. Lisää testejä tulee tehdä fotoresistikerroksen laadun varmistamiseksi.

Pinnoituslaitteiston parametrien optimointi suoritettiin kaksitasoisella (two-level full factorial) koesuunnittelumenetelmällä (Design of Experiments, DOE). DOE-mallia varten suoritettiin kokeita määritellyillä parametreillä. Kokeiden tulosten perusteella luotiin malli, joka arvioi määriteltyjen parametrien vaikutuksia päällystetyn fotoresistikerroksen lopulliseen paksuuteen. Mallin perusteella voidaan esimerkiksi nopeuttaa substraattien läpimenoa pinnoitusprosessissa 80 %:lla. Koesuunnittelu-mallin toimivuus tulee vielä varmistaa tekemällä lisää testejä.

Fotoresistikerroksen ohentamisen sekä pinnoituslaitteiston parametrien optimoinnin ansiosta pystytään nopeuttamaan tuotantoaikoja ja säästämään materiaaleissa. Lisäksi ne asettavat myös mahdollisuuden tutkia ja kehittää litografiaprosessin seuraavia vaiheita. Substraatin päällystäminen fotoresistillä on vasta ensimmäinen vaihe optisen litografian prosessissa.

Avainsanat	fotoresisti, päällystäminen, optinen litografia, etsaus, DOE

Metropolia
University of Applied Sciences

Contents

Appendices

Metropolia
University of Applied Sciences

List of Symbols and Abbreviations

Micron   Micrometer

μm Micrometer

cSt   Submultiple centistokes

cp   Centipoise

RH   Relative humidity

HV   Light energy $E = h\nu = h(c/\lambda)$, where h=Plank's constant, λ=wavelength and
        c=speed of light

PR   Photoresist

PLG   Photolithography

UV   Ultraviolet

DOE   Design of experiments

VFR   Volume flow rate

RS   Rotational speed

Rpm   Round per minute

Al_2O_3 Aluminum oxide

Nm   Nanometer

Na+   Sodium ions

1 Introduction

Photolithography is one of the most important processes used in microfabrication technology. The most valuable and important devices that are used on a daily basis from the smart phone to the computer; from the display in the airport to the transparent display put in the windshield of a vehicle, where reading the data and observing the surroundings happen simultaneously, have undergone the photolithography process.

The research of this thesis was proposed by Beneq Oy (2005), which is based in Espoo. Beneq Oy is the home of Atomic Layer Deposition (ALD), and it is known globally for its thin electroluminescent displays, ALD equipment and thin film coating services. The goal of this thesis project was to examine whether it is possible to coat a thinner photoresist layer than the one used in the current process, and to optimize the parameters of the spray coating system in the photolithography process. The photoresist layer was applied to an aluminum oxide layer during photolithography process. The photoresist protects the aluminum oxide layer during other steps of the process, and it allows the transfer of images and patterns into the aluminum oxide layer. Achieving a thinner coated photoresist layer than the one currently used, would result in faster production times, material saving and set potential for investigation of the rest steps in the photolithography process.

This thesis starts with a short introduction of the photolithography process. Photoresists, substrate preparation, coating techniques and prebake are further explained to support the experimental part of the thesis. The experimental part of this project mostly focusses on conducting tests of different thickness layers of photoresist necessary for protecting the aluminum oxide layer during the etching process. Two series of tests with two different photoresist viscosities were performed and the thickness of the coated layers was examined. The quality of the aluminum oxide layer was inspected after the etching process. Finally, the parameter optimization of the spray coating system was done using a full factorial two-level design of experiments (DOE).

2 Photolithography

The word lithography refers to the process invented in Germany in 1796 by Aloys Sene-felder (1, p. 4; 2). Photolithography comes from the Greek for the words light (photos), stone (lithos) and to write (gráphein). It literally means writing on the stones, photo was added to the term when sunlight was involved in developing (1, p. 4; 3). One of the first example of photolithography was made in 1827 by the Parisian engraver Lemaitre. He made an etched copy of the engraving of Cardinal (Figure 1), which was initially developed by the French inventor Nicéphore Niépce. (1.)

Figure 1.   Engraving of Cardinal d'Amboise. First photolithography done with wet etching (1, p. 1).

Photolithography has been on a continual development with the increased demand for smaller sizes, especially since the 1960s when the microelectronics industry used it as an important process in creating transistors (4, p. 3).

Photolithography process starts with a temporary coating of a substrate with a needed layer of photoresist (positive or negative) followed by baking. The substrate is then exposed to UV light through a mask changing the chemistry of the exposed areas. Successively a selected developer, commonly a base solution is used to remove the exposed areas (positive photoresists) or unexposed areas (negative photoresists). The pattern on the mask is finally transferred into the substrate by removing the areas that are not protected by the photoresist during the etching process (5).

Photolithography involves several typical steps in transferring the desired image into the substrate. These steps, a few of which will be explained in this thesis are substrate

preparation, coating, prebake (softbake), alignment and exposure, post-exposure bake, development, etching and stripping (Figure 2) (6, p. 13).
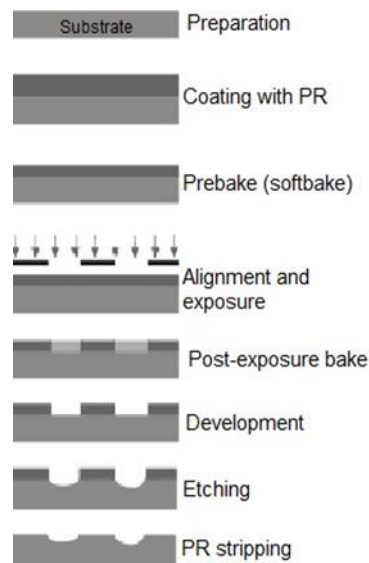

Figure 2. Typical arrangement of steps in photolithography, illustrated for a positive resist. (Photo material adapted from the book *Optical Lithography* (6, p.2), text addition and modification are done by the author).

2.1 Photoresists

Photoresist is a light-sensitive organic polymer, which is the heart of the masking process especially in microsystems technologies and microelectronics for the construction of µm and nm structures. When the photoresist is exposed and developed, it transfers the image on the aligned mask to the substrate. (7; 8.)

2.1.1 Photoresist Types

The photoresist (PR) is considered positive when the exposed areas are dissolved during the development and negative when the exposed areas are not altered by the developing process (9). With positive PR, UV light is exposed directly to the intended regions to be removed. The chemical structure of the exposed regions changes, making these regions soluble during development. The chemical change does not occur in the unexposed areas and so are left insoluble (Figure 3, left). Negative photoresists have the opposite

behavior, they are soluble in developer and the chemical structure of the exposed regions is changed from un-polymerized (soluble) to polymerized (insoluble) during the exposure. (Figure 3, middle) (10; 11, p. 4.)

There are also image reversal resists, which can be used as positive or negative mode. When it is used as positive, the process order is the same as for the positive resist. When it is used as a negative resist, few steps are done to achieve the reversal image. After the first exposure (resist behaves as a positive resist), a reversal bake is executed to cross-link the exposed regions as unexposed regions stay photo-active. Second exposure is completed without the mask (flood exposure), to change the unexposed regions from the first exposure from insoluble to soluble in the developer. After the development, the regions that were exposed in the first exposure remain as the designed pattern (Figure 3, right). Using a positive PR in image-reversal process, the result is a negative image of the mask and vice versa using a negative PR. (12, p. 54.)
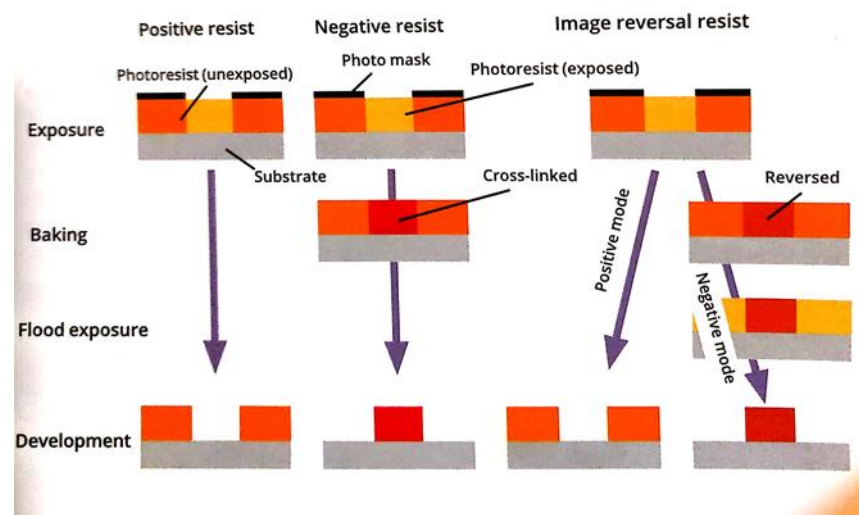

Figure 3. Process steps are demonstrated from exposure up to development using positive PR, negative PR and image reversal PR (from left to right) (12, p.54).

Photoresists are manufactured and tuned for a variety of applications for both general and specific purposes, and they must meet numerous requirements such as high sensitivity, high contrast, good adhesion, good etching resistance, good resolution and long shelf life (1, p. 40).

Table 1.   List of polymers used to produce different types of resist, which react to different exposure sources (13, p. 206).

Resist	Polymer	Polarity	Sensitivity (Coul/cm^2)	Exposure Radiation
Positive	Novolak (M–Cresol-formaldehyde)	+	$3-5 \times 10^{-5}$	UV
Negative	Poly Isoprene	–		UV
PMMA	Poly–(Methyl Methacrylate)	+	5×10^{-5}	E-Beam
PMIPK	Poly–(Methyl Iso-propenyl Ketone	+	1×10^{-5}	E-Beam/ Deep UV
PBS	Poly–(Butene-1–Sulfone)	+	2×10^{-6}	E-Beam
TFECA	Poly–(Trifluoroethyl Chloroacrylate	+	8×10^{-7}	E-Beam
COP (PCA)	Copolymer–(α–Cyano Ethyl Acrylate–α– Amido Ethyl Acrylate)	–	5×10^{-7}	E-Beam X-Ray
PMPS	Poly–(2-Methyl Pentene-1–Sulfone)	+	2×10^{-7}	E-Beam

As shown in Table 1 photoresists are modified to respond to certain wavelengths of light and different exposure sources (light, heat radiation, and so on). Optical resists are tuned to react to UV light and laser beams and others react to X-rays or electron beams (13, p. 204).

2.1.2   Photoresist Composition

A photoresist typically consists of three main ingredients; polymer (base resin), sensitizers or photoacid generators and a casting solvent. These PRs are two-component systems, whereas resists without sensitizers are one-component systems. Photoresists may also include other components (additives) such as adhesion promoters and anti-oxidizing agents. Other substances can also be included, for example, some dyed ab-sorbents might be added to the resists for easier and faster visual inspection of the coating. (1, p. 26; 12, p. 38-40.) A modern PR may contain of (by weight) 50–90 % solvent, 10–40 % resins, 1–8 % sensitizers or photoacid generators, and less than 1 % additives (14, p. 182).

Polymers are light- and energy-sensitive solid organic material, which forms the matrix of the developed resist structures. The formed layer protects the substrate from chemical or physical attacks, and it makes the transfer of the designed pattern on the mask to photoresist and subsequently to the substrate possible. A phenol-formaldehyde polymer,

also known as the phenol-formaldehyde Novolak resin (Figure 4) and a diazonaphttoqui-none (DNQ) sensitizer (Figure 5) are found in almost all positive and image reversal photoresists. (12, p. 38-39; 13, p. 205.)
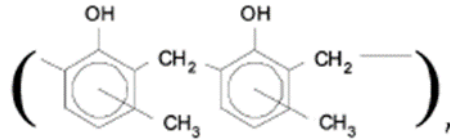

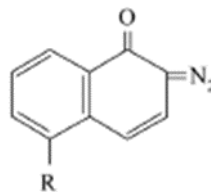Figure 4.   Structural formula of phenolic resin (14, p. 69).

Figure 5.   Structural formula of diazonaphttoquinone (DNQ) (14, p. 69).

Novolak resin is generally soluble in aqueous basic solutions, such as NaOH, KOH, or tetramethylammonium hydroxide (TMAH) in water. On the other hand, the sensitizer (DNQ) in the photoresist is insoluble in these solutions. Therefore, mixing sufficient quantity of DNQ with resin makes the PR insoluble (Figure 6) or it dissolves at exceptionally low rates in basic solutions. (14, p. 69.)
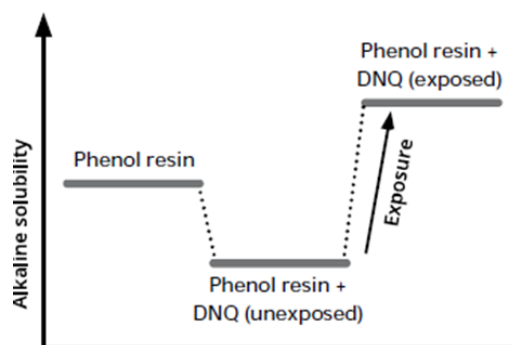

Figure 6.   Alkaline solubility of phenol resin, phenol resin mixed with DNQ (unexposed) and phe-nol resin with DNQ (exposed). The addition of DNQ reduces the alkaline solubility of phenol resin but after exposure the alkaline solubility is significantly increased (12, p. 39).

DNQ is referred as a photoactive compound (PAC), because it reacts to light (14, p. 68). To make the photoresist soluble, it has to be exposed. During exposure DNQ re-acts photochemically to UV light of a proper wavelength in a reaction known as photolysis. During photolysis reaction (Figure 7), the nitrogen is being eliminated by absorbing a photon to form a ketocarbene. After a rearrangement the ketocarbene transforms into a ketene. Within the film, if water is available, the ketene will undergo a reaction to finally convert into indenecarboxylic acid, which is soluble in aqueous solutions of hydroxide ions.
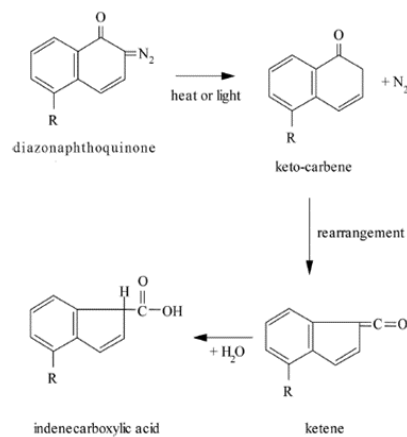

Figure 7.   Base-insoluble sensitizer (DNQ) undergoes photolysis to form indenecarboxylic acid (14, p. 69)

It is important to have water available in the film; otherwise, the ketene may react directly with phenolic resin producing cross-links. Cross-linking is highly undesirable in positive resists, because it is a negative resist behavior. (1, p. 27; 14, p. 68-69; 15, p. 297.) To make sure sufficient quantity of water is available within the resist film, it is important to let the photoresist rehydrate after the prebake step. This allows the heated film to absorb water molecules from the atmosphere of the cleanroom. (12, p. 78.) Most negative PRs have polyisoprene as a polymer (Figure 8) and biazide photoreactive cross-linker (Figure 9).
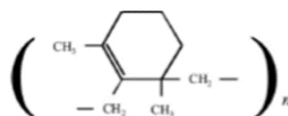

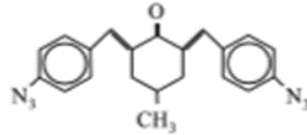Figure 8.   Structural formula of polyisoprene (14, p. 52).

Figure 9. Structural formula of biazide (14, p. 52)

During polymerization the exposed areas to UV light physically form a cross-link with amine (Figure 10), which becomes insoluble in developer and is etch resistant. (13, p. 204-205; 14, p. 51-52.)
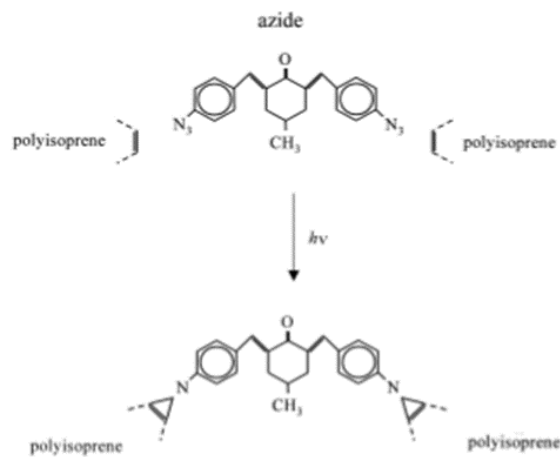
Figure 10. The cross-linking (under light energy hv) of cyclic polyisoprene with help of a commonly used azide (14, p. 52).

Image-reversal PRs are used to produce high-resolution and undercut profiles when developed. Like positive PRs, they are mostly composed of a phenol-formaldehyde Novolak resin and a diazonaphthoquinone (DNQ) sensitizer. It is also possible to use negative PRs to reverse the image. A typical image-reversal positive tone photoresist process starts with exposure to produce the carboxylic acid (Figure 11). After it has been patterned, an amine vapor is diffused into the exposed areas in a vacuum oven to neutralize the acid.
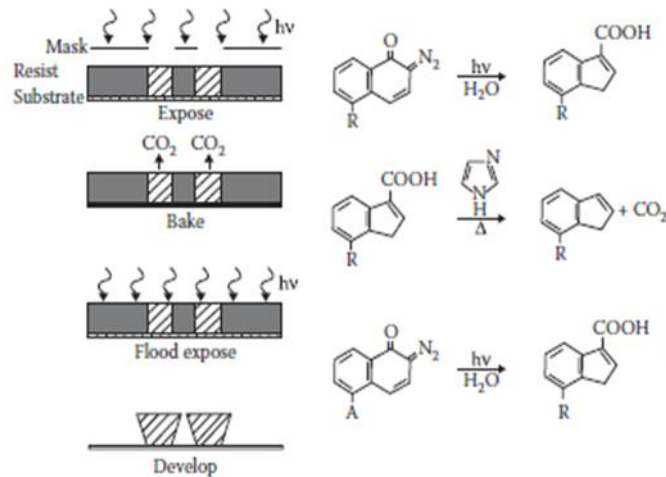
Figure 11. Image-reversal process structure with a positive PR (1, p. 51).

The resist undergoes another exposure without any mask (flood expose) to change the photochemistry of the unexposed areas in the first exposure, thus converting into carboxylic acid and the neutralized areas remain highly resistant to the second exposure and insoluble in developer. The flood exposed areas next to neutralized areas are now soluble in positive resist developers. The result is a negative image of the mask, which is intended for positive PRs.

This type of image-reversal process is sometimes favored over typical negative resist process because it is possible to achieve undercut profile (Table 2a) and improved resolution unlike the negative resists that might swell during development. (1, p. 50-51; 13; p. 317-318.)

Table 2.   Different resist profiles and uses are achieved after development, by means of positive and negative photoresists (γ=resist contrast, R is the development rate of the exposed region, R0 is the development rate of the unexposed region) (1, p.47).

Profile	Dose	Developer Influence	R/R_0	γ	Uses
(A) Positive resists undercut (a) 95–110°	High (often with backscatter radiation)	Low	>10	>6	Ion implant; liftoff; not good for plasma etching; often only obtained through image reversal
Vertical (b) 75–95°	Normal dose	Moderate	5–10	<4	Liftoff; reactive ion etch; wet etch; ion beam etch; perfect fidelity
Normal or overcut (c) 45–75°	Low	Dominant	<5	<3	Typical for positive resists; wet etch; metallization; <20% resist loss
(B) Negative resists undercut	Dominant	Little influence	<0.1	<3	Permanent resists; larger devices; MEMS

Another crucial component of photoresists is solvent; in fact, it is the largest ingredient by volume in a PR. Solvents are liquids that do not ionize; therefore, they are neutral on the pH scale. A solvent makes the resist into a liquid, and it defines the viscosity of the resist and thus allows it to be applied to surfaces with different coating techniques. Ethoxyethyl acetate or 2-methoxyethyl are main solvents in most positive PRs and in negative PRs the solvent is usually xylene, an aromatic type (13, p. 47; 2, p. 6.) As shown in Table 3 solvents with different boiling points, evaporation rates and viscosities are available for use. Photoresists can be diluted with one or two solvents of different properties to achieve a homogenous and smooth resist film layer (12, p. 39).

Table 3. Most popular resist solvents currently in use with exception of few that are considered unsafe (15, p. 185).

Chemical and common names and formula	Boiling point (°C)	Viscosity (cP)	Comments
2 Ethoxymethyl acetate (Ethyl cellusolve acetate) $C_2H_5O(CH_2)_2$ $OCOCH_3$	156	1.2	Widely used in the past, but now considered unsafe
2 Methoxyethylether (Diglyme) $CH_3OCH_2CH_2OCH_2CH_2OCH_3$	162		Widely used in the past, but now considered unsafe
Ethyl lactate $CH_3CH(OH)COOC_2H_5$	154	2.4	Currently commercially available and considered safe
Propyleneglycol monoethylether acetate (PGMEA) $CH_3O(CH_2)_2CH_2OCOCH_3$	146	1.2	Currently commercially available and considered safe
Methylmethoxy propionate $CH_3O(CH_2)_2COOCH_3$	145		Currently commercially available and considered safe
Ethyl pyruvate $CH_3COCOOC_2H_5$	155		Currently commercially available and considered safe
2 Heptanone $CH_3(CH_2)_4COCH_3$	121		Currently commercially available and considered safe
2 Ethylethoxy propionate $CH_3CH_2O(CH_2)_2COOC_2H_5$	170	1.1	Used often as cosolvent in currently commercially available solvents.
Diacetone alcohol (4 Hydroxy 4 methyl 2 pentanone) $CH_3COCH_2C(OH)(CH_3)_2$	168	2.9	Safe solvent, but not currently in use for positive resists
Cyclohexanone $(CH_2)_5O$	157	2.0	Safe solvent, but not currently in use for positive resists
Amyl acetate $CH_3COO(CH_2)_4CH_3$	142	0.8	Used only as cosolvent. Although considered safe, it is not currently in use for positive resists

2.2 Substrate Preparation

Before coating the substrate with a PR, cleaning the substrate from chemical impurities and dust particles is important. These particles and impurities will disturb the uniformity of the coated photoresist surface or can cause problems in the following processes. (16; p. 6.)

This following example of calculating the particles on the surface of an exposed substrate to air in a Class 10 clean room is adapted from the book *Manufacturing techniques for Microfabrication and Nanotechnology* (1, p. 6); if a 125-mm diameter wafer is unprotected for one minute from an air stream under a laminar flow condition at 30 m/min, this will result in 128 particles being landed on the wafer. Since there are 350 particles of 0.5 microns or larger per cubic meter in a Class 10 clean room, the air volume that passes over the substrate in one minute [(30 m/min) *π*(0.125m/2)2*1 min] is 0.368 m3. The dust particles in the air volume that passes over the substrate are 350*0.368=128 particles. Of these particles, only a portion are adhered to the substrate surface. And only a fraction of those particles adhered are at a location that might cause a failure.

Metropolia
University of Applied Sciences

Nevertheless, the clean room has an enormous impact on the quality of the patterned images. The smaller the parts that need to be patterned, the cleaner the room has to be.

Also, a removal of the desorption of water and a treatment with an adhesion promoter is recommended to maximize the adhesion between the substrate and the resist during coating. (12, p. 50; 15, p. 5.) These steps are not essential for all coating processes. If the substrates have been in the room temperature for a long period of time prior to the coating process, they have most likely absorbed water molecules from the air. For the desorption of water molecules, a bake-out is recommended at approximately 120 ˚C for a few minutes. With increase of the bake-out temperature to around 140 ˚C and above, it will also promote the adhesion of PRs to oxidized surfaces such as oxidized Si, glass, quarts and most metals. On the other hand, if the substrates have been cleaned or heated immediately in the previous process, this step is not essential.

The substrate could be either covered with dust particles or contaminated with organic impurities. The substrate can be rinsed in isopropanol to remove the particles with no further action required. In case of substrates contaminated with impurities, a two-stage cleaning is recommended. Firstly, the substrates are cleaned with acetone to remove the organic impurities followed by isopropanol to remove the contaminated acetone.

After dehydration, an adhesion promoter can also be applied to improve the adhesion and make substrate surface hydrophobic from polar OH bonds that are formed during the long exposure to air humidity. The substrates are introduced to a vapor of an adhesion-promoter, the most widely used promoter is hexamethyldisilazane known by its acronym HMDS. Said promoter binds to water-free surfaces by binding its Si atom to the oxygen atoms on the oxidized substrates surfaces releasing ammonia (Figure 12). HMDS promoting agent increases photoresist adhesion to oxides, polysilicon, quartz, nitrides and glass. (1, p. 41; 12, p. 50-51; 13, p. 220; 14, p. 55.)
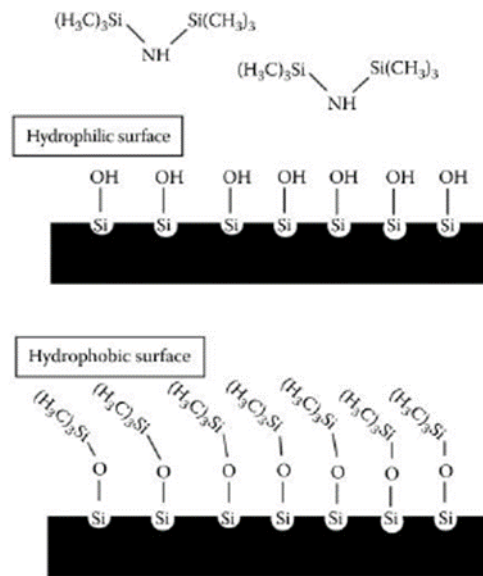
Figure 12. HMDS-promoter bonds to surface by binding its Si atom with OH releasing ammonia (1, p. 41).

2.3 Coating Techniques

Photolithography starts traditionally with the coating of a substrate. Substrates require a resist film of a well-controlled thickness, which sequentially should meet certain criteria; thickness homogeneity, film roughness, coating time, resist yield, size, geometry and weight of the substrate. On the basis of selected criteria, a coating method such as spin, spray, dip, electrodeposition, meniscus, roller, curtain… is considered to achieve the desired thickness of a layer. (6, p. 4; 12, p. 54-55; 16, p. 8.)

2.3.1 Spin

Spin-coating technique is the most widely used method because of its high potential homogeneity and throughput (12, p. 58). Spin-coating systems are constructed in manual, semiautomatic and automatic (13, p. 222). Photoresist is typically applied in a liquid form and its viscosity can be altered with a selected solvent, the higher the solvent content in the resist the lower the viscosity of the resist. As Figure 13 demonstrates the PR is deposited in the center of the substrate, which is held on a spinner chuck by vacuum (1, p. 16).
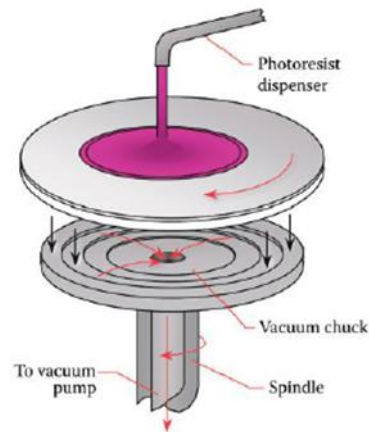
Figure 13. Photoresist spinner (1, p. 16).

The supply of the PR in the spinner is either static with the substrate at rest, or dynamic with the substrate rotating (14, p.458). In the static dispensing (Figure 14), the puddled PR in the center of the substrate is let to spread covering most of the surface. When the spread resist reaches a specified diameter, the chuck is accelerated to a programmed speed. During spinning at high speeds ranging typically 1500-6000 rmp, centrifugal force starts to spread the PR to the substrate edges and over, forming a uniform layer. (13, p. 223.)
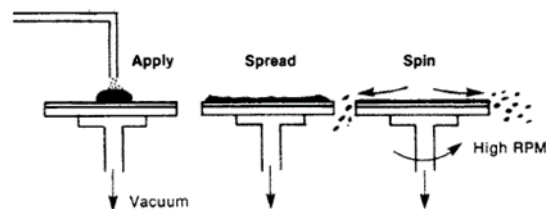
Figure 14. Static spin dispensing and acceleration of the chuck (13, p. 222).

On a stationary substrate, the resist will spread to a certain diameter. A dynamic spin dispense technique was developed to obtain a uniform resist layer on large diameters (13, p. 223). After the substrate is held in place by the vacuum chuck, a low speed of approximately 500 rmp is used. The resist is being dispensed onto the center as the substrate rotates (Figure 15). The rotation helps the spread of the resist to a larger diameter, also less resist is needed. After the dispensing, the spinner is accelerated to

high speeds to complete the spread and thin the fluid to near its final desired uniform film.
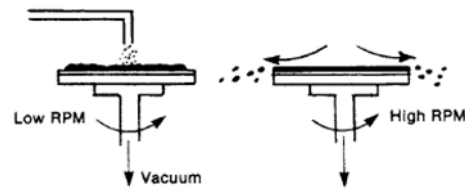
Figure 15. Dynamic spin dispensing (13, p .224).

To coat even larger diameter substrates, an improvement on the dynamic dispensing is possible by adding a moving-arm resist dispenser (Figure 16). The arm moves slowly from the center toward the edges of the substrate, forming more uniform initial and final layers. (1, p. 17; 13, p. 223.)
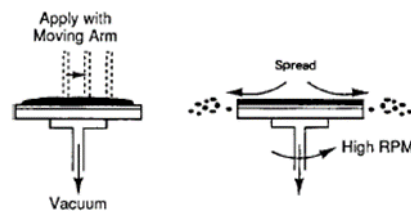
Figure 16. Moving-arm dispensing (13, p. 224).

The amount of PR dispensed in the mentioned processes is important, too much will result in a build-up of resist around edges commonly known as edge beads and too small amount will result in an incomplete resist coverage (13, p. 222). In modern spinners, these edge beads are removed with a solvent mostly by automatic EBR (edge bead removal) as shown in Figure 17.
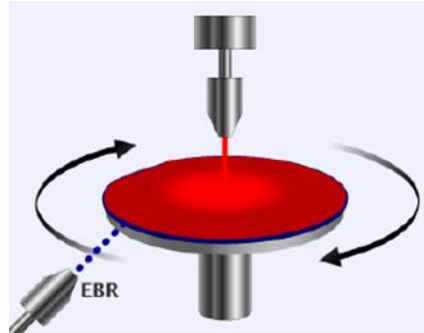
Figure 17. Removal of edge beads (17, p. 2).

After a desired film thickness is achieved, and most of the solvent has evaporated from the resist, the EBR solvent is sprayed on the edges of the spinning substrate (low speeds) to eliminate the excessive build-up. (17, p. 2.) The final film thickness is defined based on the substrate and the combination of selected time and spin speed, which in turn are programmed depending on the properties of the PR. (1, p. 16).

Some advantages of spin coating include the availability of the equipment and range of resists it uses, because of the process's wide usage, especially in microelectronics. The short coating times, film thickness homogeneity and throughput make the process prevalent. Number of parameters that affect the final film thickness is relatively low; therefore, it is easy to optimize the process. Since significant amounts of the solvent is lost during spinning, this reduces delays in the following lithography process steps for instance softbake. There are also some limitations for example if the substrate does not have a rotational symmetry, the formation of edge beads increases significantly due to air turbulence.

Even though the fast-drying times are appreciated in many projects, it could also have a negative impact in some nanotechnologies that require some time to self-assemble. Spin coating has low material usage of approximately 10 %, the rest is spun off. However, the resist that is spun off is either reused or transferred for other purposes such as being reused as a protective layer on the substrate (12, p. 58; 18, p. 81-82; 19.)

2.3.2 Spray

Direct spray coating is another coating method that is widely used in addition to spin coating. Typically, in spray coating substrates pass under a spray gun, which is either static or dynamic depending on the system and the substrate that is coated (Figure 18a). With dynamic scanning, in old spray systems the spray gun moves on a constant speed back and forth on x-axis with substrates passing under (y-axis). A constant speed is not preferable because the area requiring PR coating gets smaller as the spray gun moves closer to the middle of the substrate. In modern spray coaters, the scanning speed of the spray gun changes as it moves across the substrate to achieve a more uniform thickness film. Also, the substrate might spin under the spray nozzle at slow speeds (to minimize the centrifugal forces) as the spray gun is simultaneously moved across the substrate (Figure 18b).
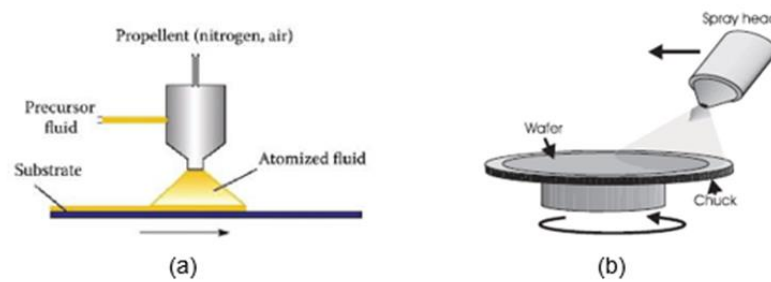
Figure 18. Photoresist deposition using spray coating alternatives (a) Substrate passes under the spray gun, which is either stationary or moving (1, p. 18), (b) substrate spins under the spray gun, spray head is moved across the wafer (20, p. 2).

The direct spray system includes a nitrogen-filled or an ultrasonic spray nozzle, which generates a supply of droplets in a micron range. The PR is brought to the nozzle from a (pressured) tank via supply pipes. Also, a pump can be installed between the tank and the nozzle to supply the PR. As shown in Figure 19, the formed droplets are carried and landed on the substrate by nitrogen or air flow. (1, p. 17-18; 12, p. 65; 20, p. 2.)
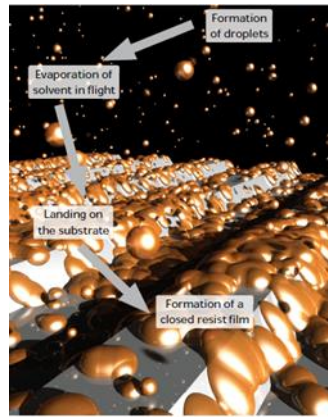
Figure 19. Transformation of atomized resist droplets to a closed resist layer (12, p. 65).

It is important that some of the solvent is evaporated during the journey between the spray nozzle and the substrate to achieve a resist edge coverage. Nevertheless, if too much solvent evaporates during flight, the formation of a closed film layer macroscopically is inhibited. Figure 20 shows the formation of a smooth, closed resist film on a non-textured silicon wafer. (12, p. 65-67.)
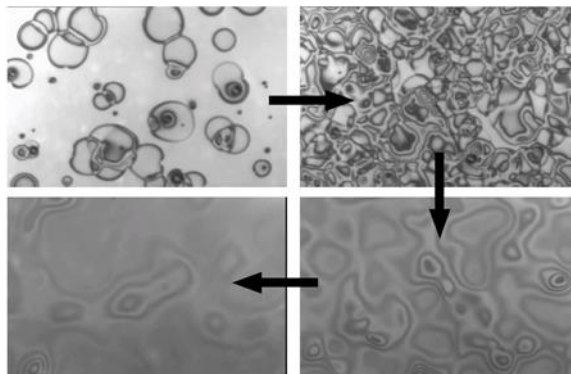
Figure 20. Formation of a resist film using spray coating (photo adapted from reference 12, p. 67).

There are numerous adjustable parameters that define uniformity, quality and the final thickness of a PR film in spray coating compared to spin coating, some of the most important ones are:

- Speed of the substrate passing under the nozzle or spinning velocity of the substrate. The faster the substrate passes under the spray head, the thinner the

formed photoresist layer will be. Spinning velocity of the substrate affects the uniformity of the layer.

- The volume of dispensed PR, which is controlled by the supply pump. The dosage affects the thickness of the PR layer. Greater the dosage, thicker the layer.

- Photoresist composition, i.e. solids content and the amount of the solvent in the PR. A desired viscosity of the PR can be achieved by adding a selected solvent.

- The scanning speed of the spray head over the substrate. Lower speeds will typically result in thicker layers.

- Distance between the spray nozzle and the substrate

- The spray pressure, which impacts the droplet size of the PR.

- One of the important parameters, which does not necessarily affect the final thickness of the photoresist is the transfer efficiency. Transfer efficiency (TE) is a measure of the actual coating material that is deposited on the substrate with respect to the total volume supplied. Improvements in TE will reduce waste disposal and costs.

Proper adjustment and understanding of these parameters are vital to achieve desired results. (20, p. 2.) Spray coating is favorable over spin and other coating methods, especially when thick photoresist layers are desired. In spray coating the resist does not build up at the edge of the substrates unlike spin coating, this allows of multi-layer coatings and results in a thick PR layer with a reasonable uniformity. The thickness variation caused by directional effect of spinning especially in substrates with cavities, does not occur with spray coating.

Coated layers applied by spray and spin methods on substrates with cavities (Figure 21), shows some striation in the spin coated layer that is caused by the thickness variation compared to the uniformity of the spin coated layer. The coating of arbitrarily shaped and textured substrates with grooves, sidewalls and edges is theoretically possible with spray

coating while spin coating does not provide required properties of the final layer. (12, p. 65; 18, p. 6; 21, p. 4.)
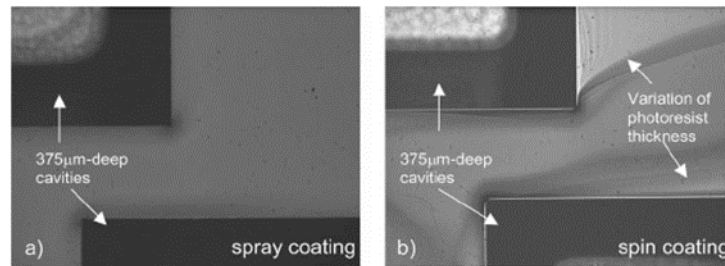
Figure 21. Wafer coated with photoresist using spray and spin coating (21, p. 4).

However, there are limitations in spray coating. For instance, as mentioned earlier substrates with cavities show less striation in spray coating than spin coating, but this is not the case if cavities with different sizes are present on the substrate. The resist at the bottom of a small cavity is thicker than in a large cavity, which leads to thickness variation. Consequently, the resolution of the patterns that need to be printed might be affected when using the same amount of exposure energy. (18, p. 3.) Also, thick resist films lead to greater times in the following steps of lithography.

The formation of a thin and closed layer of PR less than a micron is difficult to achieve due to the landing locations of the droplets following a statistical distribution. Number of variables that contributes to formation of the final layer thickness is greater than in spin coating, which makes the optimization of spray coating process difficult. (12, p. 65.) After applying the desired PR layer, the following processes in the photolithography will be determined based on the thickness of the PR layer on the substrate, except for etching, which is determined based on the layer that needs to be patterned.

2.4   Drying, Postbake and Rehydration

After coating, it is important to let the substrates dry before baking, especially when the substrate is coated with a thick PR layer. As Figure 22 illustrates, letting the substrates to dry before baking allows the solvent molecules that are present in the PR layer to diffuse first to the top of the layer before they can evaporate. If coated substrates with a

thick layer are baked immediately, this might dry the resist surface very fast, trapping the solvent within the layer leading to form bubbles and ultimately resulting in poor adhesion.
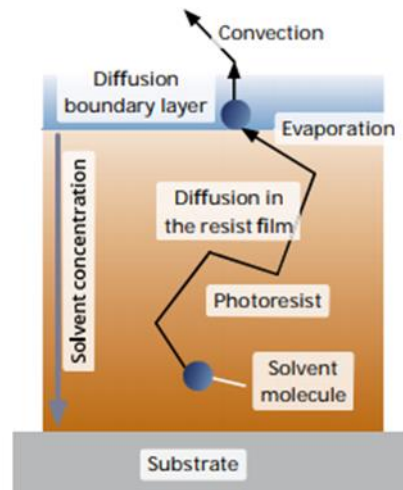
Figure 22. Illustration of a solvent molecule leaving the photoresist layer. It starts with diffusion in the resist film, evaporation, diffusion in the boundary layer just above the resist surface before it is carried away by air stream (12, p. 71).

After some solvent has evaporated in the clean room, a softbake is necessary to re-duce the remaining solvent concentration of 10–35 % (Figure 23) to preferable concentration of 5 % or below.
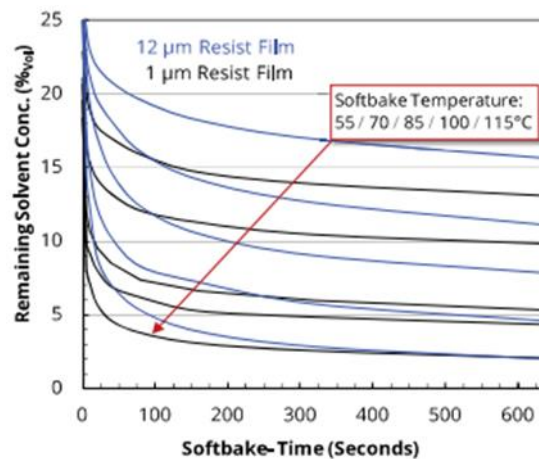
Figure 23. Impact of temperature and time on the remaining solvent concentration of 1-micron and 12-micron film thickness (12, p. 72).

Some of the benefits of a low solvent concentration in the baked layer are improving the resist adhesion, preventing nitrogen popping during exposure, avoiding the contamination of the photomask with resist and minimizing the dark erosion during development.

After prebake, the substrates should be kept at room temperature for some time to allow the resist film to rehydrate. During rehydration, the water molecules available in the air of the room are diffused through the resist film to the substrate. As can be seen in Figure 24, the time it takes for the substrate to rehydrate depends on the layer thickness and air humidity. The presence of water in the layer is important for the photolysis reaction to occur during exposure. (12, p. 71-80.)
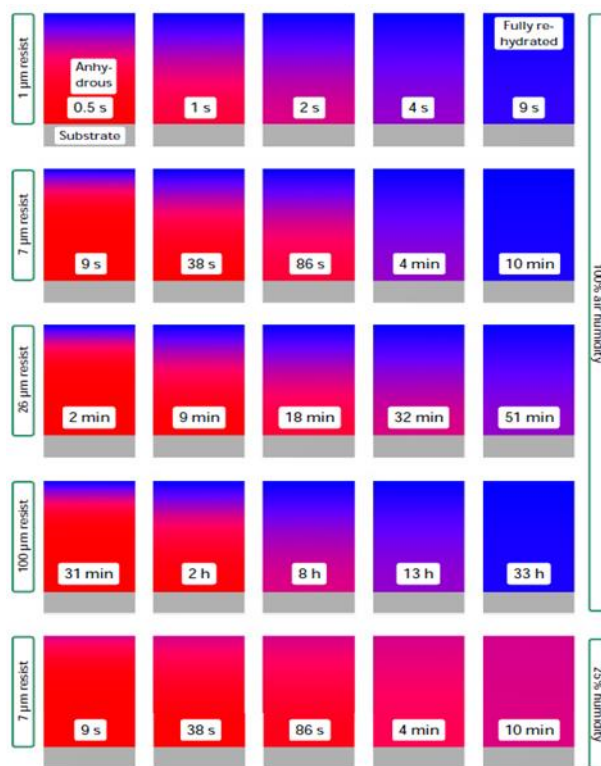
Figure 24. Rehydration time to attain water concentration in the resist based on the thickness and humidity (12, p. 79)

3   Experimental Materials and Methods

All the tests that are discussed in this section were done at Beneq Oy. Approaching this experiment, few goals were set that were equally important. The first goal was to find a suitable and closed photoresist layer (preferably as thin as possible), which will protect the selected patterned aluminum oxide layer from cavities after a selected etching process. In the current process, the aluminum oxide layer is coated with a photoresist layer of approximately 16-17 microns. Since the photoresist would be diluted with a solvent, the goal was to use as little solvent as possible in the dilution. Lastly, the parameters of the spray system, where the tests were done to be optimized.

3.1   Materials

The tests were performed on 63 rectangle glasses, which were 195Wx265Lx1D mm of size. First, the glass substrates were passivated with an aluminum oxide (Al_2O_3) layer of 27 nm to prevent the Na+ ions present on the glass surface from accessing the thin films. The substrates were then sputtered with a pure aluminum layer of 100 nm to make the inspection of the cavities in the Al_2O_3 layer possible during the etching process, since Al_2O_3 is transparent. Lastly, another Al_2O_3 layer of 80 nm was added on the top of the pure aluminum layer. The quality of the substrates was inspected before the experiments.

During the spray coating, 74 plain glasses (same size of the substrate) were used before initial tests. A positive photoresist (AZ4533) was used in the experiments, which is suitable for achieving thick photoresist layers. Said photoresist had a solids content of 34.5 %, a high viscosity of 125 cSt at 25 ˚C and spectral sensitivity of 310 – 440 nm according to the manufacturer. Coating with a spray system requires photoresists with low viscosities; therefore, the photoresist was diluted with an AZ EBR solvent. The solvent was over 98 % of 1-methoxy-2-propanol acetate. The substrates were developed with a NaOH-based solution, etched with an Al-etchant and the remaining photoresist was removed with selected PR strippers.

3.2   Methods

Coating

The spray system had a dynamic spray gun that moved at a constant speed rate back and forth at the x-axis, while the substrates passing under the spray gun in one direction on a belt (y-axis) at a speed rate that could be adjusted (Figure 18a). The system had a nitrogen-filled nozzle, to which the PR supply pump was also attached. The pressure of the nitrogen and the volume flow rate of the supply pump were adjustable. Before coating, the substrates were heated in an oven at 100 ˚C for 5 - 10 minutes to desorb the water molecules that might have been absorbed in the cleaning room and to improve the adhesion of the PR to the surface of the substrate as discussed in 2.2 substrate preparation.

Drying, prebake (softbake) and rehydration

After the coating, the substrates were kept in the clean room (20–22 ˚C) for minimum of 30 minutes. For prebaking, a temperature of 100 ˚C for 2-10 min/micron resist film thickness is recommended for the photoresist in a convection oven according to the manufacturer. The exact thickness of the coated resist layers was still unknown during softbake, they would theoretically range based on the used parameters between 5–40 microns. The substrates were softbaked firstly at 70 ˚C for 5 min, then the temperature was increased to 100 ˚C for 30 min and followed by another 5 min at 70 ˚C.

After the softbake, the substrates were kept in the clean room (20–22 ˚C and 45 RH%) for at least 30 minutes to rehydrate. This method of drying, softbake and rehydration was conducted for all the tests regardless of the thickness of the layers.

Alignment and Exposure

The first part of this step was the alignment of the substrate with the photomask, which had the image (Figure 25) to be patterned into the PR layer. The photomask was held on a vacuum chuck with a photomask holder above. The substrate and the mask are usually marked with a symbol to ensure exact alignment. During alignment, the locations of the marks were viewed through a split-field objective microscope. Then the chuck was

moved manually until the substrate was aligned with the mask. After alignment, the substrate was moved automatically under the UV lamp to be exposed and was returned to the starting point.

The substrates were exposed with an i-line exposure system with a 365 nm wavelength that is suitable for the used positive photoresist with a spectral sensitivity of 310 – 440 nm. The exposure was performed using a mask aligner with a proximity projection meaning there is a small gap (in microns) between the resist and the mask. An expo-sure energy dose of 1000 mJ/cm2 was applied to all the substrates regardless of the layer thickness. A post exposure bake was not necessary for the selected positive photoresist.

Development and etching

The substrates were developed from 8 minutes to 30 minutes depending on the layer thickness. It was rather easy to inspect the substrate surface to see whether the resist layer was developed or needed more time.

Unprotected areas were removed (etched) by an Al-etchant, transferring the image permanently into the Al2O3 surface layer. After etching, the remaining photoresist on the pattern was removed with selected photoresist strippers followed by drying of the substrates.

3.3   Experiments

Three series of tests were executed; For the first series of tests, the photoresist was diluted with the solvent with a ratio of 3:1, while for the second series, the photoresist was diluted with the solvent with a ratio of 2:1. The absolute viscosity of the dilutions was measured with a digital rotational viscometer. The spindle of the viscometer was kept at a constant speed at 60 rpm for 3 minutes, while immersed in the photoresist. The goal of these two series of tests was to find a suitable PR layer to protect the aluminum layer free of cavities during the etching process. The quality of the aluminum layer (how many cavities are etched into it) was inspected visually by placing the substrate on top of a lamp. In case there was a hole in the layer, the light would come through.

The third series of tests were done for the optimization of the spray system using design of experiments (DOE) method. Few of the parameters that have an impact on the final thickness of the PR layer were not possible to adjust, and these parameters were kept constant for all the tests that were done in the spray system.

In the first series of tests, two different set of tests were done with photoresist and solvent dilution of 3:1, which had a viscosity of approximately 38 cp. In the first tests, spray pressure was set at 7 bar and the rotational speed of the PR supply pump was 18 rpm based on the current process. The speed of the belt (how fast the substrates passed under the spray gun) was changed as shown in Table 4 (left). In the second part of the tests, the spray pressure was set at 7 bar, the speed of the belt was set at 26 cm/min and the and the rotational speed of the PR supply pump was changed as shown in Table 4 (right).

Table 4.   Speed rates of the belt with constant rotational speed of PR supply pump of 18 rmp and spray pressure of 7 bar (left). Different dispensed volume flow rates via supply pump by changing its rotational speed (RS) and constant belt speed of 26 cm/min and spray pressure of 7 bar (right) were performed.

Run	Belt speed (cm/min)
1	26
2	29
3	32
4	35
5	38
6	41
7	44

Run	RS (rpm)
1	12
2	14
3	16
4	18
5	20
6	22
7	24

In the second series of tests, also two different set of tests were done with photoresist and solvent dilution ratio of 2:1, which was approximately 20.5 cp of viscosity. The first tests were performed by changing the belt speed exactly the same way as in Table 4 (left). In the second tests, the spray pressure was set at 7 bar and the belt speed was set at 47 cm/min based on the current process setup. The dispensed volume via sup-ply pump was changed as shown in Table 5.

Table 5.   Different pumping rates (RS) of dispensed photoresist with constant belt speed of 47 cm/min and spray pressure at 7 bar were examined.

Run	RS (rpm)
1	18
2	17
3	16
4	15
5	14

For the optimization of the spray coating system, for example how parameters affect the final thickness layer and how they interact with each other, a design of experiments (DOE) was executed using a full factorial two-level design. On the basis of the earlier series of tests that were done, factors of belt speed (A), volume flow rate of the dispensed PR (B) and nitrogen-filled nozzle pressure (C) were chosen for a 2k factorial experiment design (k=number of factors).

Rest of the parameters were kept constant for all the runs. For each factor, mini-mum and maximum values were chosen as shown in Table 6 as coded (left), actual values (middle) and the runs were done in a random order (right). Also, a series of three tests was performed using the center points of the factors.

Table 6.   Coded (left) and actual (middle) values that were used in a random order (right) in the DOE.

Run	A	B	C
1	-1	-1	-1
2	-1	-1	1
3	-1	1	-1
4	-1	1	1
5	1	-1	-1
6	1	-1	1
7	1	1	-1
8	1	1	1

Run	A	B	C
1	26	12	6
4	26	40	8
6	47	12	8
7	47	40	6
2	26	12	8
3	26	40	6
5	47	12	6
8	47	40	8

Run	A	B	C
1	26	12	6
2	26	12	8
3	26	40	6
4	26	40	8
5	47	12	6
6	47	12	8
7	47	40	6
8	47	40	8

All the substrates were marked with numbers and symbols before coating. Two substrates were used per test and before each test two plain glasses were used. Coating the plain glasses first allowed the spray system to become steady and also the parameters to be adjusted before coating the actual substrates. One substrate would go to development, which would then be measured for the thickness of the PR layer. The other substrate of the same test would go all the way through the etching process and be inspected for cavities and overall quality of the aluminum oxide layer. This method was used for all the tests except for DOE. The only difference with the DOE test series was that only one substrate was coated since only the final thickness was of interest.

Thickness of the PR layers was measured with a DEKTAK Veeco 200Si surface texture measuring system. The system measures the surface electromechanically by moving the sample beneath a diamond-tipped pen, which is mechanically joined to the core of a linear variable differential transformer (LVDT). The measurement started on the top layer near the patterned image edge, crossing the edge line to the bottom layer calculating the height difference (top layer thickness). Three locations on the substrate were measured for PR layer thickness as shown in Figure 25.
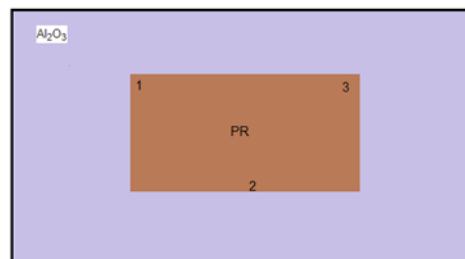
Figure 25. Surface of a substrate with a photoresist patterned image on an aluminum oxide layer after development. The thickness of the PR layer was measured from the three locations on the image (1,2 and 3)

4   Results and Discussion

4.1   Thickness and Quality

The results from the photoresist and solvent dilution ratio of 3:1 series from Section 3.2.1 are presented graphically in Figure 26 (see Appendix 1&2 for detailed measurements). As can be expected from Section 2.3.2, the thickness of the PR layer decreases with increasing the speed rate of the substrates passing under the spray gun (Figure 26 left). While increasing the volume of the dispensed photoresist via the supply pump increases the thickness of the layer (Figure 26 right).
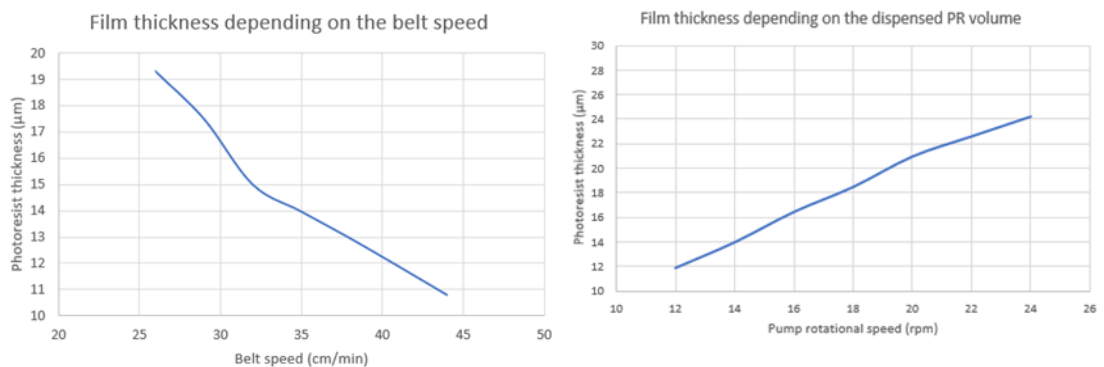
Figure 26. Thickness of the PR layer decreases, when belt speed is increased (left), while the thickness increases with increasing the volume of the dispensed photoresist using a direct spray gun system (right).

The results from the photoresist and solvent dilution ratio of 2:1 are presented graphically in Figure 27 (see Appendix 3&5 for detailed measurements). As can be seen, the results are similar to those that were achieved with the dilution of 3:1. Thickness de-creases with increasing the speed rate of the belt (Figure 27 left). While thickness in-creases with increasing the flow rate volume of the dispensed photoresist (Figure 27 right).
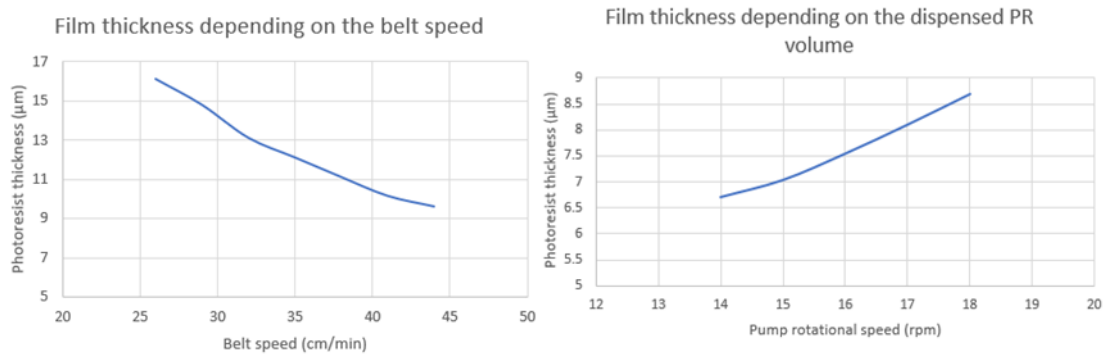
Figure 27. Thickness of the PR layer decreases, when belt speed is increased (left), while the thickness increases with increasing the volume of the dispensed photoresist using a direct spray gun system.

Although the speed rate of substrates passing under the spray gun and the amount of the dispensed photoresist have a similar impact on the final thickness layer. Different layer thicknesses were achieved with different dilution of the photoresist as it can be noticed in Figure 28 that is based on the first series of the tests with both dilutions. All the parameters were the same; spray pressure at 7 bar, RS of supply pump at 18 rpm and the belt speed was changed for both dilutions as presented in Table 4 (left). With the photoresist of lower viscosity (dilution 2:1), thinner film layers were achieved.
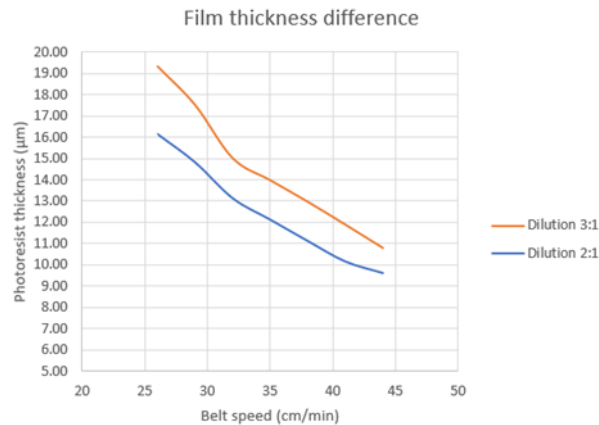
Figure 28. Different thicknesses are achieved using different photoresist viscosities in the spray coating system.

Although thick resist layers were achieved with the higher viscosity of the 3:1 ratio, the quality, however, was not as expected. In Figure 29, on the left side is a picture of a developed photoresist pattern. The thickness of the said photoresist layer was approximately 17.5 microns, which is rather thick in lithography standards. In the middle picture of Figure 29 is a magnified image of a cavity that occurred in the aluminum oxide layer on the substrate despite the protection of the 17.5 microns thick layer. On the right side of Figure 29 is a magnified picture of two cavities close to each other, which were etched into the aluminum layer protected with a 12 microns thick photoresist layer during the etching process. Number of cavities (Table 7) were noticed in the aluminum oxide layer with photoresist dilution of 3:1.

Figure 29. 17.5 µm thick photoresist layer (yellowish layer) after development (left). A 24 µm cavity in length in the aluminum oxide layer, which was coated with the 17.5 µm thick photoresist layer (middle). Two cavities of approximately 30 µm in length each in the aluminum oxide layer, which was coated with 12 µm PR layer (right).

Table 7. Number of cavities noticed in the aluminum oxide layer after the etching process in the test series of 3:1 dilution.

Average PR layer thickness (µm)	Number of cavities in Al_2O^3 layer
19.30	0
17.49	1
15.00	2
13.97	1
12.96	0
11.89	2
10.80	0

Diluting the photoresist with more solvent in the ratio of 2:1 resulted in better quality after the etching process. As can be seen in Figure 30 the size of the hole is smaller, approximately 15 microns in diameter. Even more importantly cavities occurred in the aluminum layer only with low developed PR layer thickness of 8.7 microns and less (Table 8). With layers of 7 microns and thinner, the small holes started to become trickier to count and they were labelled as bad quality.
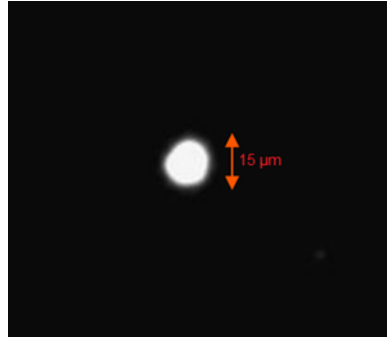
Figure 30. Magnified image of a cavity in the aluminum oxide layer, which is around 15 microns in diameter. The protecting PR layer was around 8.7 microns thick during etching.

Table 8.   Number of cavities noticed in the aluminum oxide layer in the test series of 2:1 dilution.

Average PR layer thickness (µm)	Number of cavities in Al_2O^3 layer
16.14	0
14.81	0
13.15	0
12.14	0
11.15	0
10.17	0
9.65	0
8.70	1
8.10	2

On the basis of the results of the tests presented in Table 8, there were no cavities in the aluminum oxide layer that was protected with a 9.65 µm PR layer during the etching process. This experimental photoresist layer is thinner than the one in the current process of approximately 16-17 µm. The decrease in the PR film thick-ness will result in saving materials and faster process times, when the experimental PR layer enters the production. More tests should be done with same thickness of the films to guarantee the reliability and consistency of the aluminum oxide layer quality after the etching process.

Lower viscosity is preferable for spray coating as was expected from Sections 2.3.2 and 3.2. The Solvent impacts the size of the droplet distribution during coating, which allows flow of the droplets and converging of the film on the substrates leading to a closed and smooth film. However, if diluted further with solvent, it might lead to a non-closed film, since the solvent evaporates during the drying and the prebake. Too much solvent in the photoresist also leads to long baking times and increases the dark erosion rate during

development. These issues should be investigated with doing more tests. (12, p.176-177.)

4.2 Design of Experiment (DOE)

On the basis of the first experiments, the factors of belt speed, dispensed PR volume and nitrogen-filled nozzle pressure have the most impact on the final thickness layer. Therefore, these were chosen for the DOE. Photoresist viscosity also has a great impact on the final thickness and on basis of the previous tests and results, it was noticed that the photo-resist and solvent dilution of 2:1 had the better quality. This dilution of 2:1 was also used in the DOE runs. The thickness measurements of the DOE runs are presented in Table 9 and results of the center points are shown in Table 10 (see Appendix 5&6 for detailed measurements).

Table 9.   Thickness measurements achieved with the design of experiment runs based on three factors: belt speed, rotational speed of the supply pump and nitrogen pressure with photoresist dilution ratio of 2:1.

Run/Substrate	Belt speed (cm/min)	Pump rotational speed (rpm)	Pressure (bar)	Average PR layer thickness (µm)
1	26	12	6	10.85
4	26	40	8	38.91
6	47	12	8	5.72
7	47	40	6	19.54
2	26	12	8	10.08
3	26	40	6	36.60
5	47	12	6	5.71
8	47	40	8	19.71

Table 10. Thickness measurements of center points of the factors: belt speed, RS of supply pump and nozzle-filled nitrogen pressure with photoresist dilution ratio of 2:1.

Run/Substrate	Belt speed (cm/min)	Pump rotational speed (rpm)	Pressure (bar)	Average PR layer thickness (µm)
1	36.5	26	7	16.22
2	36.5	26	7	16.29
3	36.5	26	7	16.36

The results were added to Minitab, which calculated the factors' impact on the final thickness. For the DOE used, the software would calculate/present how much of an impact both a single factor or an interaction of factors has on the final response (thickness), the impact direction (positive or negative) and a model for response optimization. The magnitude and the importance of the effects on the thickness can be seen in Figure 31. The longer the bar, the more impact the factor or interaction of factors has on the response.
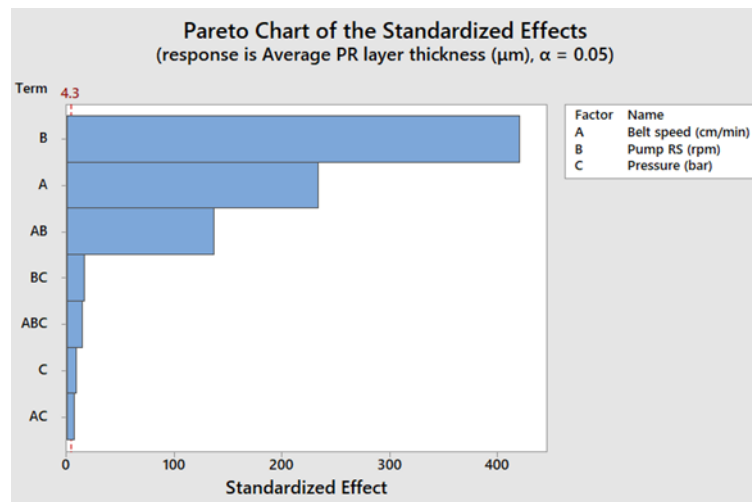
Figure 31. Factors and their interaction impact on the PR layer thickness.

On the basis of the eight tests of DOE and three tests of the center points, the three factors with the most impact on the thickness are rotational speed of the supply pump (B), belt speed (A) and their interaction (AB). The single factor with least impact is the nozzle-filled nitrogen pressure (C) followed by its interaction with belt speed (AC). The direction, magnitude and the importance of the factors are shown in Figure 32.
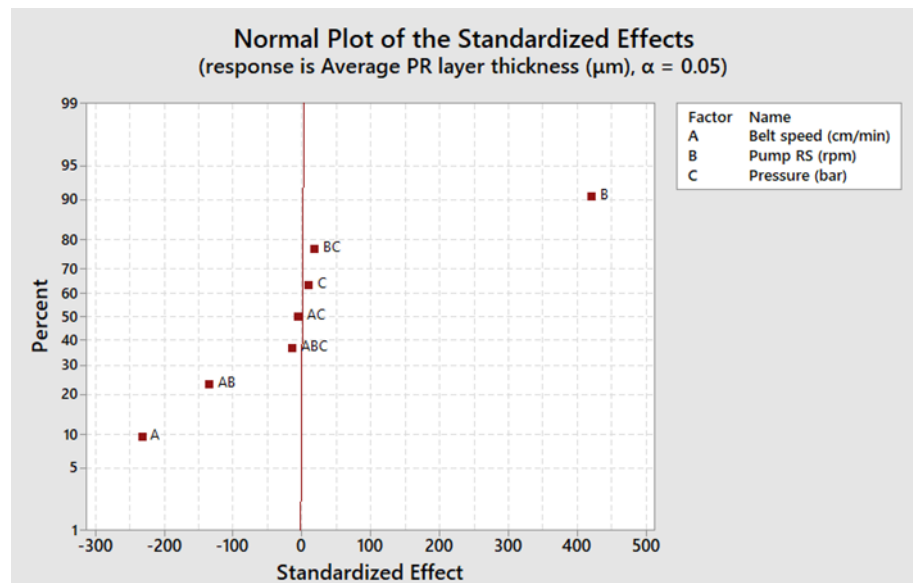
Figure 32. Magnitude, direction and the importance of the factors on the layer thickness. The factors and interactions that are far from the reference line are considered significant.

As it can be seen in Figure 32, the belt speed (A) has a negative effect, which means changing the factor from high level to low level will result in a higher response (thicker layer). On the other side (positive side), is the rotational speed of the supply pump (B), which has even larger impact (further from the reference line) on the response. It has a positive effect, which means increasing the VFR of the photoresist via the supply pump from low level to high level will result in a thicker layer. This was also noticed in the earlier measurements and results (Figure 26). Factors and interactions that are near or on the reference line (0 effect) are considered insignificant.

Minitab software has a response optimizer tool that is very effective and useful for analyzing large data especially for factorial designs. It calculates an optimal solution and draws a plot for the stored model. In the plot, a targeted response can be added, and it will calculate the optimum values of the factors. These values can be modified interactively to determine how different values affect the response.

For example, a response (layer thickness) can be determined with the model generated based on the DOE tests that were performed. As shown in Figure 33, a targeted response of 16 microns is desired (current process), a pressure of 7 bar and a belt speed of 47 cm/min is put for fast coating (26 cm/min in current process). The optimizer will

then calculate the rotational speed of the supply pump, which is approximately 33.75 rpm.
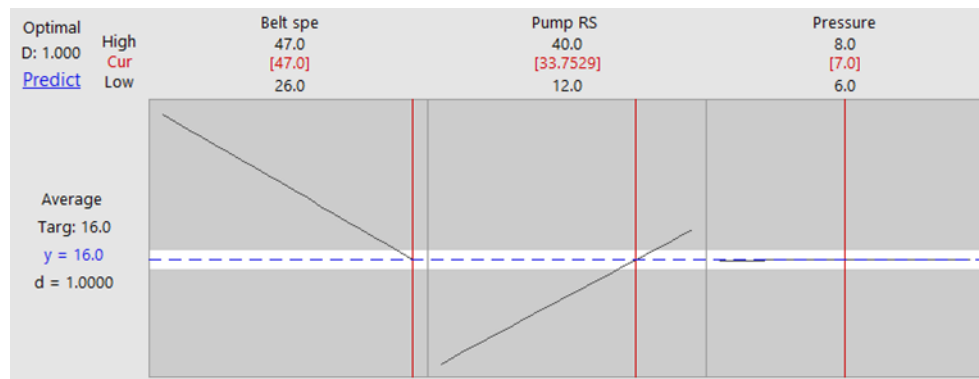
Figure 33. Optimization plot for rotational speed of the PR supply pump by adjusting the factors of belt speed to 47 cm/min, pressure to 7 bar and a desired layer thickness at 16 microns. (y=response and d = desirability)

Theoretically, the coating rate of the substrates can be increased by 80 %. In the above model, there are only the 11 tests in total (8 tests for DOE and 3 tests for center points). Thickness of the PR layers was set as the response in the model. Therefore, more tests should be done with parameter setups based on the model to further increase its reliability and consistency, and the quality of the aluminum oxide layer to be inspected.

In Figure 34, the model is tested for reliability using the optimizer tool. Three different responses are achieved by adjusting all values of the factors to center points (in red font). In the top model, the results of the center points from Table 10 are put in the model as center points. In the middle model, the center points are considered as extra tests. In the bottom model the center points are removed completely (see Appendix 8 for input data).
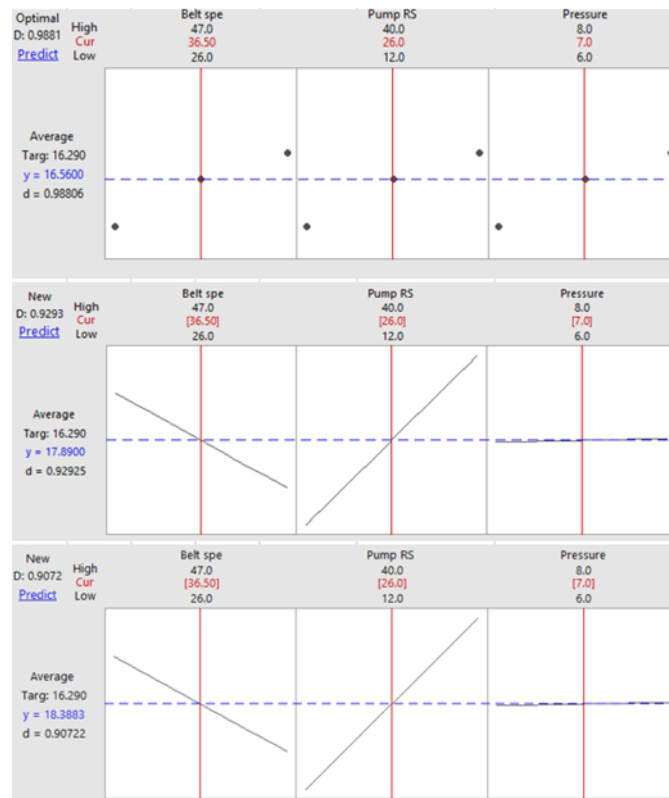
Figure 34. Prediction of the layer thickness (=response in blue font) based on three models with factors set at their mid values. In the top model, center points (Table 10) are put as center points (8 DOE tests + 3 center points), in the middle model, the center points are considered as extra tests (11 DOE tests) and in the bottom model, the center points are removed from the model (8 DOE tests).

On the basis of the measurements of the center points in Table 10, an average thickness of approximately 16.29 microns was achieved. From the models above, the most reliable is the top model, which has the closest response of 16.56 microns. However, there is a limitation in Minitab with model optimization that has center points. The optimizer considers only the high, low and the center points of each factor as can be seen in Figure 34 (top). For example, if one factor is moved to its high value, the rest of the factors will also be moved to their high values. For the optimization of the spray coating system with a variable response, the second model (Figure 34 middle) can be used for optimization. By doing more tests and adding the thickness results to the model will further increase its reliability. By adding the measurement results of the tests that were performed in the first series (Table 4) to the model, a better response of 17 microns was achieved.

5   Conclusions

The decrease of approximately 38 % in the thickness of the photoresist layer can successfully be used in aluminum oxide layer protection during the etching process, which will result in saving materials and faster production times in the photolithography process. More tests should be done to further increase reliability of the process and consistency of the layer.

With the photoresist of low viscosity, thinner photoresist films with fewer cavities in the aluminum oxide layer can be achieved. Hence, further diluting of the photoresist with the solvent and usage of photoresists with low viscosities can be examined.

On the basis of the optimization of the spray coating system, the speed of the substrates passing in the coating system can be increased by 80 %. More tests should be done with setups based on the model; thus, the quality of the aluminum oxide layer is guaran-teed. Few important parameters of the coating system were not adjustable, therefore upgrading machinery parts would further increase opportunities to optimize the system.

Photoresist coating is the first step in the photolithography process, and the subsequent steps of the process need to be modified accordingly. The possible thinning of the photoresist layer and the parameter optimization of the spray coating system set potential for further development and investigation of other lithography process steps.

References

1. Madou MJ. Fundamentals of Microfabrication and Nanotechnology: Manufacturing Techniques for Microfabrication and Nanotechnology. 3rd ed. CRC Press; 2011.

2. COLOR PRINTING: LITHOGRAPHY [Internet]. [cited 2019 Mar 6]. Available from: http://www.lib.udel.edu/ud/spec/exhibits/color/lithogr.htm

3. photo- | Origin and meaning of photo- by Online Etymology Dictionary [Internet]. [cited 2019 Mar 9]. Available from: https://www.etymonline.com/word/photo-#etymonline_v_14897

4. DavidG. Bucknall, editor. Nanolithography and patterning techniques in microelectronics. Boca Raton: CRC Press; 1385. 302 p.

5. Lin Q. Properties of photoresist polymers. In: Physical properties of polymers. 2nd ed. New York: IBM Thomas J. Watson Research Center, 1101 Kitchawan Rd, Route 134 / P.O. Box 218, Yorktown Heights, NY 10598; 2006. p. 1061.

6. Mack C. Optical Lithography. Greivenkamp JE, editor. Bellingham: SPIE Field Guides; 2006. 500 p.

7. The Basics of Microlithography [Internet]. [cited 2019 Mar 15]. Available from: http://www.lithoguru.com/scientist/lithobasics.html

8. What are photoresists composed of, and how do they work? - Allresist EN - ALLRESIST GmbH – Strausberg, Germany [Internet]. [cited 2019 Mar 16]. Available from: http://www.allresist.com/faq-photoresists-composition/

9. Soyano A. Application of polymers to photoresist materials. Int Polym Sci Technol. 2012;39(5):33–9.

10. The Difference Between Positive and Negative Photoresist | Shin-Etsu MicroSi [Internet]. [cited 2019 Mar 16]. Available from: https://www.microsi.com/the-difference-between-positive-and-negative-photoresist/

11. Tomicic D. Adhesion measurements of positive photoresist on sputtered aluminum surface. Sci Technol. 2002.

12. Koch C, Rinke TJ. Photolithography Basics of Microstructuring. 1st ed. Ulm, Germany; 2017.

13. Van Zant P. Microchip Fabrication. Vol. 155, McGraw Hill Professional. 2004.

Metropolia
University of Applied Sciences

14. Okoroanyanwu U. Chemistry and Lithography. Bellingham: SPIE and John Wile & Sons, Inc.; 2010.

15. Levinson HJ. Principles of Lithography. 3rd ed. Principles of Lithography. Bellingham: SPIE; 2010.

16. Shelley MD, Zaouk R, Park BY, Madou MJ. Introduction to Microfabrication Techniques. Microfluid Tech. 2006;(June 2014):pages 3-16.

17. (SCME) SC for ME. Photoresist Thickness Activity. 2017;1–8.

18. Pham N, Boellard E, Sarro PM, Burghartz JN. Spin, Spray coating and Electro-deposition of photoresist for MEMS structures–A comparison. Adv Futur [Internet]. 2002;81–6. Available from: http://citeseerx.ist.psu.edu/viewdoc/download?doi=10.1.1.9.8031&rep=rep1&type=pdf

19. Spin Coating: A Guide to Theory and Techniques – Ossila [Internet]. [cited 2019 Apr 7]. Available from: https://www.ossila.com/pages/spin-coating

20. Pham NP, Burghartz JN, Sarro PM. Spray coating of photoresist for pattern transfer on high topography surfaces. J Micromechanics Microengineering. 2005;15(4):691–7.

21. Pham NP, Boellaard E, Burghartz JN, Sarro PM. Photoresist coating methods for the integration of novel 3-D RF microstructures. J Microelectromechanical Syst. 2004;13(3):491–9.

Appendix 1. Film thickness depending on the belt speed (dilution 3:1)

Belt speed (cm/min)	Substrate	Location on PR image	Location thickness (μm)	Average PR layer thickness (μm)
26	1	1	19.70	19.30
		2	18.92	
		3	19.27	
29	2	1	17.51	17.49
		2	18.13	
		3	16.82	
32	3	1	14.70	15.00
		2	15.50	
		3	14.80	
35	4	1	14.33	13.97
		2	12.62	
		3	14.94	
38	5	1	12.57	12.96
		2	13.72	
		3	12.59	
41	6	1	12.37	11.89
		2	11.44	
		3	11.88	
44	7	1	10.67	10.80
		2	11.06	
		3	10.67	

Appendix 2. Film thickness depending on the rotational speed of the supply pump (dilution 3:1)

Pump rotational speed (rpm)	Substrate	Location on PR image	Location thickness (µm)	Average PR layer thickness (µm)
12	1	1	12.00	11.87
		2	12.00	
		3	11.60	
14	2	1	13.90	13.97
		2	14.00	
		3	14.00	
16	3	1	16.78	16.45
		2	15.95	
		3	16.62	
18	4	1	18.44	18.49
		2	18.91	
		3	18.11	
20	5	1	21.01	20.98
		2	21.11	
		3	20.82	
22	6	1	22.79	22.63
		2	22.41	
		3	22.69	
24	7	1	24.67	24.25
		2	23.63	
		3	24.44	

Metropolia
University of Applied Sciences

Appendix 3. Film thickness depending on the belt speed (dilution 2:1)

Belt speed (cm/min)	Substrate	Location on PR image	Location thickness (μm)	Average PR layer thickness (μm)
26	1	1	16.21	16.14
		2	16.00	
		3	16.20	
29	2	1	14.40	14.81
		2	15.33	
		3	14.70	
32	3	1	13.13	13.15
		2	13.11	
		3	13.20	
35	4	1	12.20	12.14
		2	12.00	
		3	12.21	
38	5	1	11.21	11.15
		2	11.43	
		3	10.80	
41	6	1	10.40	10.17
		2	9.91	
		3	10.21	
44	7	1	9.53	9.65
		2	9.70	
		3	9.71	

Appendix 4. Film thickness depending on the rotational speed of the supply pump (dilution 2:1)

Pump rotational speed (rpm)	Substrate	Location on PR image	Location thickness (µm)	Average PR layer thickness (µm)
18	1	1	8.87	8.70
		2	8.51	
		3	8.73	
17	2	1	8.08	8.10
		2	8.41	
		3	7.80	
16	3	1	7.39	7.55
		2	7.69	
		3	7.56	
15	4	1	7.02	7.04
		2	7.08	
		3	7.02	
40	5	1	6.85	6.71
		2	6.65	
		3	6.64	

Appendix 5. Thickness measurement results for DOE

Run/Substrate	Belt speed (cm/min)	Pump rotational speed (rpm)	Pressure (bar)	Location on PR image	Location thickness (µm)	Average PR layer thickness (µm)
1	26	12	6	1	10.83	10.85
				2	10.72	
				3	10.99	
4	26	40	8	1	39.44	38.91
				2	35.60	
				3	41.68	
6	47	12	8	1	5.85	5.72
				2	5.52	
				3	5.79	
7	47	40	6	1	20.33	19.54
				2	18.71	
				3	19.59	
2	26	12	8	1	9.90	10.08
				2	10.39	
				3	9.94	
3	26	40	6	1	35.41	36.60
				2	39.38	
				3	35.02	
5	47	12	6	1	5.62	5.71
				2	5.68	
				3	5.82	
8	47	40	8	1	19.12	19.71
				2	19.99	
				3	20.02	

Appendix 6. Thickness measurement results of center points

Run/Substrate	Belt speed (cm/min)	Pump rotational speed (rpm)	Pressure (bar)	Location on PR image	Location thickness (µm)	Average PR layer thickness (µm)
1	36.5	26	7	1	16.26	16.22
				2	16.07	
				3	16.32	
2	36.5	26	7	1	16.02	16.29
				2	16.51	
				3	16.34	
3	36.5	26	7	1	16.09	16.36
				2	16.78	
				3	16.20	

Metropolia
University of Applied Sciences

Appendix 7. Model regression equation for thickness calculation

Regression Equation in Uncoded Units

Average PR layer thickness (µm) = 13.67 - 0.2920 Belt speed (cm/min) + 0.7306 Pump RS (rpm)
- 2.303 Pressure (bar)
- 0.00539 Belt speed (cm/min)*Pump RS (rpm)
+ 0.04840 Belt speed (cm/min)*Pressure (bar)
+ 0.11938 Pump RS (rpm)*Pressure (bar)
- 0.002480 Belt speed (cm/min)*Pump RS (rpm)*Pressure (bar)
- 1.8283 Ct Pt

Appendix 8. DOE data put into Minitab models with center points (top), center points as extra tests (middle) as shown in CenterPoint column and with no center points (bottom)

Belt speed (cm/min)	Pump RS (rpm)	Pressure (bar)	Average PR layer thickness (µm)	CenterPoints
47	40	6	19.54	1
26	40	8	38.91	1
47	12	8	5.72	1
47	40	8	19.71	1
26	12	6	10.85	1
47	12	6	5.71	1
26	12	8	10.08	1
26	40	6	36.60	1
37	26	7	16.22	0
37	26	7	16.29	0
37	26	7	16.36	0

Belt speed (cm/min)	Pump RS (rpm)	Pressure (bar)	Average PR layer thickness (µm)	CenterPoints
47	40	6	19.54	1
26	40	8	38.91	1
47	12	8	5.72	1
47	40	8	19.71	1
26	12	6	10.85	1
47	12	6	5.71	1
26	12	8	10.08	1
26	40	6	36.60	1
37	26	7	16.22	1
37	26	7	16.29	1
37	26	7	16.36	1

Belt speed (cm/min)	Pump RS (rpm)	Pressure (bar)	Average PR layer thickness (µm)	CenterPoints
47	40	6	19.54	1
26	40	8	38.91	1
47	12	8	5.72	1
47	40	8	19.71	1
26	12	6	10.85	1
47	12	6	5.71	1
26	12	8	10.08	1
26	40	6	36.60	1

Metropolia
University of Applied Sciences